1514 *Biochemistry* **2011,** *50,* 1514–1523
DOI: 10.1021/bi101687t

BIOCHEMISTRY
including biophysical chemistry & molecular biology
Article

Influence of C-Terminal Amidation on the Efficacy of Modelin-5

Sarah R. Dennison and David A. Phoenix*

School of Pharmacy and Biomedical Sciences, University of Central Lancashire, Preston PR1 2HE, U.K.

Received October 20, 2010; Revised Manuscript Received January 10, 2011

ABSTRACT: To gain insight into the effects of amidation on the mechanism of membrane interaction, we studied two peptides modelin-5-COOH and modelin-5-$CONH_2$ and found they exhibit high surface activities (23.2 and 27.1 mN/m, respectively). When they were tested against *Escherichia coli*, amidation was seen to increase efficacy approximately 10-fold. Our results demonstrated that both peptides adopted low levels of α-helix in solution (< 20%); however, in the presence of *E. coli* lipid extract, modelin-5-$CONH_2$ had a greater propensity (69%) than modelin-5-COOH (32%) to generate α-helical structure. The binding coefficient for both peptides was ∼10 μM, and the Hill coefficient approximated 1, suggesting that for both peptides the interactions with *E. coli* membranes were monomeric and comparable in strength. The peptides showed a clear preference for anionic lipid, with monolayer data showing that enhanced levels of helicity were associated with a greater pressure change (∼6 mN/m). Use of fluorescein-phosphatidylethanolamine showed the amidated version was able to generate greater levels of membrane disruption, which was confirmed by thermodynamic analysis. The data would imply that both peptides are able to initially bind to bilayer structures, but upon binding, the amidation stabilizes helix formation. This would be expected to help overcome a key rate-limiting step and generate higher local concentrations of peptide at the bilayer interface, which in turn would be predicted to increase efficacy.

Antimicrobial peptides (AMPs)[1] selectively target microorganisms to protect the host. Their precise mechanism of action is not known, but they are lipid interactive and thought to target lipid components of the bacterial cell membrane leading to membrane disruption (*1*−*3*). In general, studies have focused on peptides that adopt an α-helical structure and have led to a number of models for describing the antimicrobial action of these peptides, for example, barrel stave (*1*), torroidal pore (*4*), and carpet mechanism (*5*). Subtle differences in the lipid composition of the target cell membrane are known to result in differences in the susceptibility of cells to individual peptides and may even influence their mode of action (*6*, *7*). For example, in contrast to eukaryotic cells, bacterial membranes contain a high level of negatively charged phospholipids such as phosphatidylglycerol (PG) and cardiolipin (CL) (*7*), and interaction with these anionic moieties is thought to be key for the effective function of many AMPs.

Structurally modified residues appear to play a role in the structure−function relationships of AMPs. One of the most common post-translational modifications is C-terminal amidation (*8*), which occurs naturally in a wide variety of peptides produced by Australian tree frogs such as aureins, caerins, citropins, and maculatin (*9*, *10*). C-Terminal amidation also occurs naturally in other peptides such as dermaseptin (*11*), melittin (*12*), and cecropins (*13*). There have been a number of studies of the biological significance of this structural modification, and it has been attributed a number of actions (*8*, *14*). Some authors have suggested that C-terminal amidation can prevent the enzymatic degradation of AMPs (*15*). Other authors have observed that the propensity for peptides to adopt α-helical structure appears to be strongly favored by C-terminal amidation and have argued that this is due to the provision of an additional hydrogen bond for α-helix stabilization (*16*, *17*). It has also been proposed that the increased positive charge given to peptides by C-terminal amidation improves the efficacy of their antimicrobial action (*18*), and this has been postulated to be due to enhanced electrostatic interactions with membrane components. Consistent with this suggestion, it has been shown that amidated dermaseptin s3 exhibited an increased potency of up to 10-fold against a range of microorganisms in comparison to the nonamidated isoform (*19*), and indeed, amidation was found to be key with respect to the lytic activity of the peptide (*11*). Studies on the β-sheet peptide, indolicidin, have also showed that C-terminal amidation improved the activity of the peptide by facilitating better lipopolysaccharide binding and thereby self-promoted uptake across the outer membrane (*20*).

In the search for new antibiotics, several groups have modified naturally occurring antimicrobial peptides and attempted to increase specificity (*8*) by systematically modifying the sequence to alter properties such as charge, hydrophobic moment, amphiphilicity, and sequence length (*21*). Modelin-5 (KLAKKLAKLAKLAKAL) is a member of a large family of synthetic antimicrobial peptides that have been used to investigate the structure−activity relationship of AMPs (*22*). The primary sequences of modelin variants contain multiple combinations

*To whom correspondence should be addressed: Office of the Vice Chancellor, University of Central Lancashire, Preston PR1 2HE, U.K. Phone: +44 (0) 1772 892504. Fax: +44 (0) 1772 892936. E-mail: daphoenix@uclan.ac.uk.

[1]Abbreviations: *A*, area per molecule in the monolayer; AMPs, antimicrobial peptides; α, interaction parameter; CL, cardiolipin; C_s^{-1}, compressibility modulus; DOPE, dioleoyl-*sn*-glycero-3-phosphoethanolamine; DOPG, dioleoyl-*sn*-glycero-3-phosphoglycerol; FPE, fluorescein-phosphatidylethanolamine; ΔH, mixing enthalpy; ΔG_{mix}, Gibbs free energy of mixing; K_d, binding coefficient; MIC, minimal inhibition concentration; PE, phosphoethanolamine; PG, phosphatidylglycerol; PBS, phosphate-buffered saline; Π, surface pressure.

 Published on Web 01/17/2011

of hydrophobic and hydrophilic amino acids ranging from 9 to 17 amino acid residues in length, and this family of peptides has been shown to have antimicrobial activity against a broad spectrum of microorganisms (*22*, *23*). In this work, we have investigated the impact of amidation on the function of modelin-5.

EXPERIMENTAL PROCEDURES

Materials. All phospholipids were purchased from Avanti Polar Lipids (Alabaster, AL) and were used without further purification. Solvents were obtained from VWR (HPLC grade). Modelin-5-COOH (KLAKKLAKLAKLAKAL-OH) and modelin-5-$CONH_2$ (KLAKKLAKLAKLAKAL-NH_2) were synthesized by Pepceuticals (Leicestershire, U.K.) by solid state synthesis and purified by HPLC to >95% purity. Buffers and solutions for monolayer experiments were prepared from Milli-Q water with a specific resistance of 18 MΩ cm. All other reagents were purchased from Sigma.

Antimicrobial Activity of Modelin-5-COOH and Modelin-5-$CONH_2$. Cultures of *Escherichia coli*, strain W3110, which had been freeze-dried in 20% (v/v) glycerol and stored at −80 °C, were used to inoculate 10 mL aliquots of sterile nutrient broth. These samples were then incubated in an orbital shaker (100 rpm and 37 °C) until the exponential phase (OD = 0.6; λ = 600 nm) was reached. Each cell culture was then centrifuged using a benchtop centrifuge at 15000*g* and 4 °C for 10 min. The resulting cell pellet was washed three times in 1 mL aliquots of a 25% strength Ringer's solution. The cells were then resuspended in 1 mL of a 25% strength Ringer's solution. Stock solutions of modelin-5-COOH and modelin-5-$CONH_2$ (1000 μM) dissolved in Ringer's solution were used to double dilute each peptide from 1000 to 3.90 μM in 1 mL aliquots. These 1 mL aliquots of peptide solution were separately inoculated with 10 μL of the cell suspension and incubated at 37 °C overnight in an orbital shaker (100 rpm). As a control, bacterial cultures were similarly treated but in the absence of peptide. After incubation, aliquots (10 μL) of the peptide bacterial culture were surface-spread onto nutrient agar plates and incubated at 37 °C for 12 h. After overnight incubation, the plates were viewed and the lowest sample concentration yielding no bacterial growth was identified as the minimal inhibitory concentration (MIC).

Total Lipid Extracts from E. coli Cells. A modified protocol of the method of Bligh and Dyer (*24*) of lipid extraction was used to extract *E. coli* membrane lipids. In summary, cultures of *E. coli* were grown in nutrient broth until the exponential phase (OD = 0.6; λ = 600 nm) was reached. The cultures were then washed twice in a 25% strength Ringer's solution and centrifuged using a Jouran benchtop centrifuge at 14000 rpm to form a cell pellet. Each pellet was then resuspended in 1 mL of Tris buffer (10 mM, pH 7.5); to a 0.4 mL aliquot of this cell suspension was added 1.5 mL of a 1:2 (v/v) chloroform/methanol mixture, and then the mixture was vortexed. Water (0.5 mL) was then added and the mixture vortexed for 5 min before being centrifuged at low speed (660*g* for 5 min) to produce two phases. The lower organic layer was concentrated using a Jouran speed vac and the dried lipid extract stored at −20 °C under N_2.

Monolayer Experiments. Monolayer experiments were performed at room temperature using an 80 mL 601M Langmuir Teflon trough (NIMA Technology, Coventry, U.K.) equipped with moveable barriers. The surface pressure was measured with a Wilhelmy plate made of Whatman's CH1 filter paper. The subphase consisted of 10 mM Tris buffer (pH 7.5) prepared with Milli-Q water. To determine the surface activity of the two peptide isoforms, we used a Hamilton syringe to inject peptide via an injection port into the subphase to give final concentrations ranging between 1.0 and 12 μM in the absence of any lipid. After injection, the surface pressure increased and continued to do so for up to 30 min. The maximal values of these surface pressure changes were then plotted as a function of the peptide final subphase concentration. The ability of peptides to spread onto aqueous surfaces and form stable monolayers was determined in the Langmuir trough described above containing 10 mM Tris buffer (pH 7.5). Peptide in methanol (2.5 mM) was spread onto the aqueous surface to give 1.5×10^{15} peptide molecules and left for 10 min to allow solvent to evaporate. The barriers were compressed at a constant speed of 0.33 nm^2/min. Experiments were repeated five times and conducted at room temperature.

The insertion of the two modelin-5 isoforms into phospholipid monolayers was investigated. Monolayers were formed dropwise by spreading chloroform solutions of bacterial lipid extracts, dioleoyl-*sn*-glycero-3-phosphoglycerol (DOPG), dioleoyl-*sn*-glycero-3-phosphoethanolamine (DOPE), and *E. coli* cardiolipin (CL) using a Hamilton syringe. The solvents were allowed to evaporate for 15 min, and then the lipid monolayer was compressed at a velocity of 10 cm^2/min to give a surface pressure of 30 mN/m, where the phospholipids are packed at a density similar to that found in bacterial cell membranes (*25*). When the target pressure was reached, the surface area of the monolayer was kept constant using a build-in feedback mechanism. The film was then left to equilibrate for 10 min before stock modelin peptide solutions were injected into the subphase to give a final concentration of 6 μM. The ability of each modelin-5 peptide to interact with lipid monolayers was also investigated using compression isotherms. Monolayers were formed by spreading onto a 10 mM Tris buffer subphase to give 2.5×10^{15} phospholipid molecules in chloroform solutions. Monolayers were formed from DOPG, DOPE, and CL, and synthetic mixes were also prepared to mimic the membrane composition of *E. coli* (*7*). The lipid monolayers were allowed to settle for 30 min before the barriers were compressed at a speed of 0.22 nm^2/min until the monolayer collapse pressure was achieved. These experiments were then repeated in the presence of either 6 μM modelin-5-COOH or modelin-5-$CONH_2$. The analysis of the compressibility modulus (C_s^{-1}) was evaluated to provide more detailed information about the lipid packing within the monolayer (*26*) and defined as

$$C_s^{-1} = -A\left(\frac{\delta\pi}{\delta A}\right) \quad (1)$$

where π represents the monolayer surface pressure and A is the area per molecule in the monolayer. To improve our understanding of the miscibility between the components of the isotherm, we investigated the thermodynamic stability of monolayers by applying the Gibbs equation:

$$\Delta G_{mix} = \int [A_{12} - (X_1 A_1 + X_2 A_2)\, d\pi] \quad (2)$$

where A_n is the molecular area occupied by the mixed monolayer, A_n is the area per molecule in the pure monolayers of component n, X_n is the molar fraction of component n, and π is the surface pressure. Numerical data were calculated from the compression isotherms according to the mathematical method of Simpson (*27*).

Furthermore, the interaction parameter and mixing enthalpy were also calculated at the different surface pressures (*26*), which is given by

$$\alpha = \frac{\Delta G_{mix}}{RT(X_1X_2^2 + X_1^2X_2)} \quad (3)$$

where X is the molar fraction of the monolayer lipid component, $R = 8.314$ J mol^{-1} K^{-1}, and $T = 294$ K. The stability and binding interactions of monolayers were further investigated using the mixing enthalpy (ΔH) (*26*), which is given by

$$\Delta H = \frac{RT\alpha}{Z} \quad (4)$$

where $R = 8.314$ J mol^{-1} K^{-1}, $T = 294$ K, and Z is the packing fraction that is calculated using the model of Quickenden and Tan (*28*).

CD Spectroscopy. CD experiments were performed using a J-815 spectropolarimeter (Jasco) with samples kept at 20 °C. Far-UV CD spectra were collated for the peptide in H_2O, in a 50% TFE/H_2O mixture, and in the presence of lipid. CD experiments were also performed at peptide:lipid ratios of 1:10 and 1:100. Total lipid extracts and phospholipids (5 mg/mL) DOPG, DOPE, and CL were dissolved separately in chloroform and dried under N_2 gas. The lipid film was rehydrated using 1× phosphate-buffered saline (PBS, pH 7.5) for 1 h or until the solution was no longer turbid. The lipid suspension was diluted 10-fold using PBS. Peptide/lipid samples were prepared via addition of the stock peptide solution (final concentration of 0.1 mg/mL) to the measured volume of lipid suspension to obtain the desired peptide:lipid molar ratio before being mixed thoroughly. Four scans per sample were performed over a wavelength range of 180−260 nm at 0.5 nm intervals, a bandwidth of 1 nm, and a scan speed of 100 nm/min. The CD spectra in Figure 2 were recorded using a 10 mm path length cell. For all spectra acquired, the baseline acquired in the absence of peptide was subtracted. The percentage helical content was estimated using a method previously described by Forood et al. (*29*). These experiments were repeated four times, and the percent helicity was averaged. To determine whether there was a statistically significant difference between the percent helicity of the two peptides in the presence of each phospholipid mix, a t test was undertaken, using SPSS version 18, based on the null hypothesis that there was no difference between the mean percent helicity.

Peptide Binding to Vesicles. LUVs with a mean diameter of 0.1 μm were prepared as previously described by Wall et al. (*30*) except 0.5 mol % fluorescein-phosphatidylethanolamine (FPE) was added to the organic solvent before it was dried under vacuum for 5 h. The lipids were hydrated in 10 mM Tris-HCl (pH 7.4) and 1 mM EDTA at a total lipid concentration of 10 mg/mL, frozen and thawed five times, and extruded 11 times using a 0.1 μm polycarbonate filter using an Avanti mini-extruder apparatus. The LUVs were stored at 4 °C under nitrogen gas. FPE-labeled LUVs were diluted to 65 μM, and fluorescence was recorded using a FP-6500 spectrofluorometer (Jasco, Tokyo, Japan), with an excitation wavelength of 492 nm and an emission wavelength of 516 nm, the excitation and emission slits set to 5 nm, and analyte sensitivity set to high. The incorporation of the FPE label was checked using the methodology previously described by Wall et al. (*30*). The fluorescence change upon the addition of 10 mM $CaCl_2$ to FPE-labeled vesicles was recorded. Once the fluorescence emission intensity had stabilized, the fluorescence change followed by the addition of 3.0 μM calcimycin (A23187 calcium ionophore) was recorded. To investigate the binding of the peptide to *E. coli* membrane mimics, aliquots of each peptide (from 0 to 320 μM) were added to the FPE-labeled LUVs and the fluorescence was monitored. The change in fluorescence (ΔF) of FPE-labeled vesicles with addition of peptide minus FPE-labeled vesicles was plotted versus peptide concentration and fitted by nonlinear least-squares analysis to

$$\Delta F = \frac{\Delta F_{max}[M]}{K_d + [M]} \quad (5)$$

where [M] is the modelin concentration, ΔF is the fluorescence change, F_{max} is the maximal fluorescence change, and K_d is the binding coefficient. To determine whether there was a statistical significant difference in K_d between modelin-5-COOH and modelin-5-$CONH_2$, a t test was undertaken using SPSS version 18. The Hill coefficient was then calculated using the methodology described by Moreno et al. (*31*). To improve our understanding of the binding of both peptides to *E. coli* membranes, we recorded the fluorescence change upon the addition of 150 μM peptide to FPE-labeled vesicles. Once the fluorescence emission intensity had stabilized, the fluorescence change followed by the addition of 10 mM $CaCl_2$ and 3.0 μM calcimycin (A23187 calcium ionophore) was recorded.

RESULTS

Antimicrobial Properties of Modelin-5 Isoforms. Modelin-5 and other modelin isoforms are known to have microbicidal activity against a variety of prokaryotic microorganisms (*22*, *23*). The antimicrobial activity of the two peptides, modelin-5-COOH and modelin-5-$CONH_2$, was tested against Gram-negative *E. coli* using a standard antimicrobial assay (*32*). After 12 h, modelin-5-$CONH_2$ exhibited potent antimicrobial activity against *E. coli*, with 100% colony reduction at a peptide concentration of 31.25 μM. In contrast, modelin-5-COOH exhibited reduced antimicrobial activity against *E. coli*, with 100% colony reduction at a peptide concentration of 250 μM.

Surface Activity of Modelin-5 Isoforms. The hydrophobic and amphiphilic properties of many AMPs are usually associated with high surface activity and a high affinity for phospholipids at the membrane interface (*33*). Here, the surface activities of the antimicrobial peptides modelin-5-COOH and modelin-5-$CONH_2$ were investigated at the air−buffer interface. Figure 1A shows that for both modelin-5-COOH and modelin-5-$CONH_2$, the surface activity depends on peptide concentration. It can be clearly seen that at a modelin-5 subphase concentration of 8 μM saturation is achieved and the peptides are highly surface active with surface pressure increases of 23.2 and 27.1 mN/m, respectively, which is characteristic of membrane interactive structure (*34*). The compression isotherms for the pure peptides show that both isoforms are able to form stable monolayers (Figure 1B). Under compression, these monolayers showed collapse surface pressures in the range of 25 mN/m, indicating the presence of well-ordered peptide films (*26*). The extrapolated area at a π of 0 mN/m for these isotherms provides a measure of the mean monolayer surface area per modelin-5 molecule (*35*). In each case, the areas are close to 2.8 nm^2, which would be expected if the peptide was in an α-helical conformation, oriented horizontally to the air−water interface, and comparable to that reported for other amphiphilic peptides such as melittin (*36*).

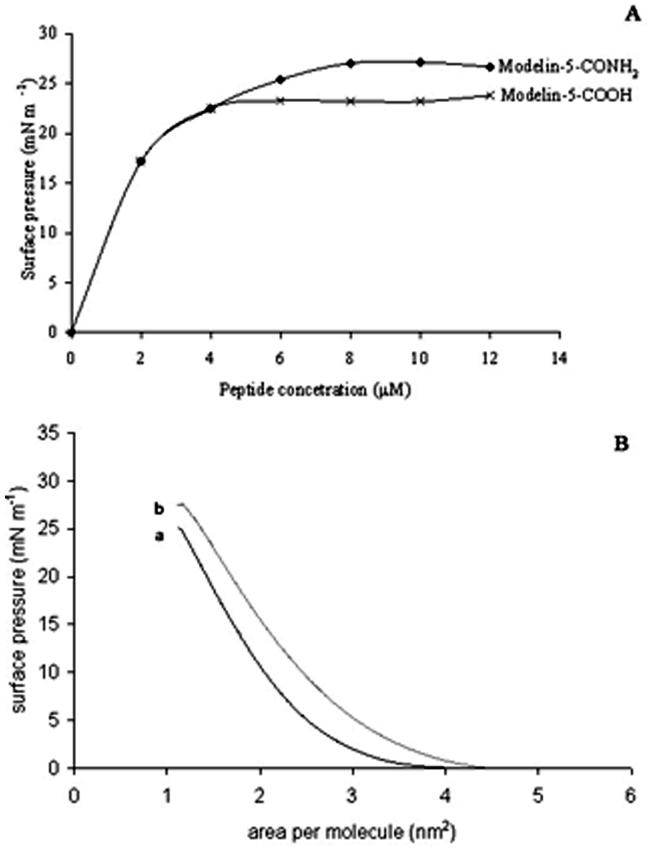

FIGURE 1: Surface activity of modelin-5-COOH and modelin-5-$CONH_2$. (A) Effect of peptide concentration of surface pressure. Surface pressure values were determined after 30 minutes of the peptide injected into the subphase. (B) Compression isotherms of modelin-5-COOH (a) and modelin-5-$CONH_2$ (b) on a 10 mM Tris pH 7 subphase. These experiments were repeated five times.

Secondary Structure of Modelin-5 Isoforms. CD spectroscopy showed that in water, modelin-5-COOH and modelin-5-$CONH_2$ exhibit spectra typical of a mixture of α-helical structure and random coil (Figure 2A). Spectral analysis showed modelin-5-COOH was 13% helical and modelin-5-$CONH_2$ 18% helical in water (Table 1). The spectrum of modelin-5-$CONH_2$ showed a significantly enhanced level of helix (100%) in the presence of TFE (Figure 2B) ($T = -2.996$; $p = 0.00$) compared to that of modelin-5-COOH (52%), suggesting that amidation has increased the propensity for the amidated peptide to form helical structure. It is widely accepted that cationic antimicrobial peptides adopt enhanced helical structure in the presence of a membrane lipid; therefore, to verify that these peptides remained in an α-helical structure in different lipid environments, we conducted CD experiments in the presence of vesicles with various lipid compositions (Table 1) and at varying peptide:lipid ratios (1:10 and 1:100). In the presence of *E. coli* lipid extracts (Figure 2C and Table 1) and a peptide:lipid ratio of 1:100, both amidated and nonamidated forms show significant increases in helical content in the presence of vesicles, with modelin-5-$CONH_2$ exhibiting approximately 2-fold higher helical content (69%) than modelin-5-COOH (32%) ($T = -2.99$; $p = 0.00$). The lipid composition of *E. coli* membranes includes 91% PE, 3% PG, and 6% CL (*7*); therefore, the helical content of the peptides in the presence of these individual components was investigated. Although PE is known to be the major component of *E. coli* membranes, CD analysis showed that both peptides were ~31% helical (Table 1) in the presence of PE vesicles (Figure 2F), and no statistically significant difference was observed between the two peptides ($T = -1.355$; $p = 0.592$). In contrast, the presence of anionic CL (Figure 2E and Table 1) induced 96% helical content in modelin-5-$CONH_2$ and 70% helical content in the case of modelin-5-COOH, showing that there was a statistically significant difference between the two peptides ($T = -2.997$; $p = 0.00$). While the helical content in the presence of DOPG (Figure 2D and Table 1) was slightly reduced for both modelin-5-$CONH_2$ (86%) and modelin-5-COOH (61%) ($T = -3$; $p = 0.00$), these results indicate that the presence of an anionic lipid can strongly initiate helix formation at the phospholipid interface.

At a 1:10 peptide:lipid ratio (Table 1), enhanced helicity was observed for modelin-5-COOH in the presence of *E. coli*, DOPG, and DOPE ($p \leq 0.00$). However, in the presence of a CL membrane, no major changes in modelin-5-COOH structure were observed ($T = -0.354$; $p = 0.738$), indicating that the peptide does not interact with CL membranes via a concentration-dependent mechanism. Enhanced helicity was also observed for modelin-5-$CONH_2$ with a 1:10 peptide:lipid ratio in the presence of *E. coli* and DOPE membranes ($p \leq 0.00$). There were no significant differences in helical content between 1:10 and 1:100 peptide:lipid ratios for modelin-5-$CONH_2$ in the presence of DOPG ($T = 0.865$; $p = 0.425$) and CL ($T = -2.190$; $p = 0.08$) membranes.

Penetration of Modelin-5 Isoforms into Phospholipid Monolayers. It is well-established that antimicrobial peptides use membrane invasion as a primary killing mechanism (*3*, *5*), and therefore, to elucidate the characteristics of modelin-5 isoform membrane interactions, we investigated the ability of the peptide to partition into a variety of pure lipid monolayers. Insertion studies were first performed on DOPE, DOPG, and CL monolayers (Figure 3). Modelin-5-COOH and modelin-5-$CONH_2$ induced maximal surface pressure changes of 4.2 and 6 mN/m, respectively, in monolayers formed from DOPG but higher maximal surface pressure changes of 4.5 and 7.9 mN/m, respectively, in monolayers formed from CL. However, a lower level of interaction was observed for DOPE monolayers in which the peptides induced surface pressure changes of 2 mN/m for modelin-5-COOH and 4.8 mN/m for modelin-5-$CONH_2$. In line with the structural data, these results indicate that modelin-5 has an affinity for anionic lipids, with the amidated version in particular showing a preference for CL. The insertion of modelin-5-$CONH_2$ into *E. coli* lipid extracts (Figure 3D) followed hyperbolic kinetics, inducing a surface pressure change of 5.9 mN/m. These high levels of interaction are consistent with disruption of the monolayer acyl chain region. However, while modelin-5-COOH also interacted with the *E. coli* lipid extract, it induced a smaller surface pressure change of only 2 mN/m, implying it is less able to penetrate into the acyl chain region.

Binding of Modelin-5-COOH and Modelin-5-$CONH_2$ to FPE-Labeled E. coli Vesicles. The incorporation of FPE into *E. coli* lipid mix vesicles was checked using $CaCl_2$ and calcimycin (A23187). Figure 4A shows the addition of Ca^{2+} ions to a suspension of FPE *E. coli* vesicles increases the fluorescence intensity, indicating that the probe is accessible in the external leaflet. Following the addition of the ionophore calcimycin (A23187), the fluorescence increased (Figure 4A) as the calcimycin allowed the Ca^{2+} to access the interior of the vesicle. The results indicate that ~66% of the probe is located in the outer leaflet, which is in agreement with previously published work (*30*). Figure 4B shows hyperbolic binding of modelin-5-COOH and

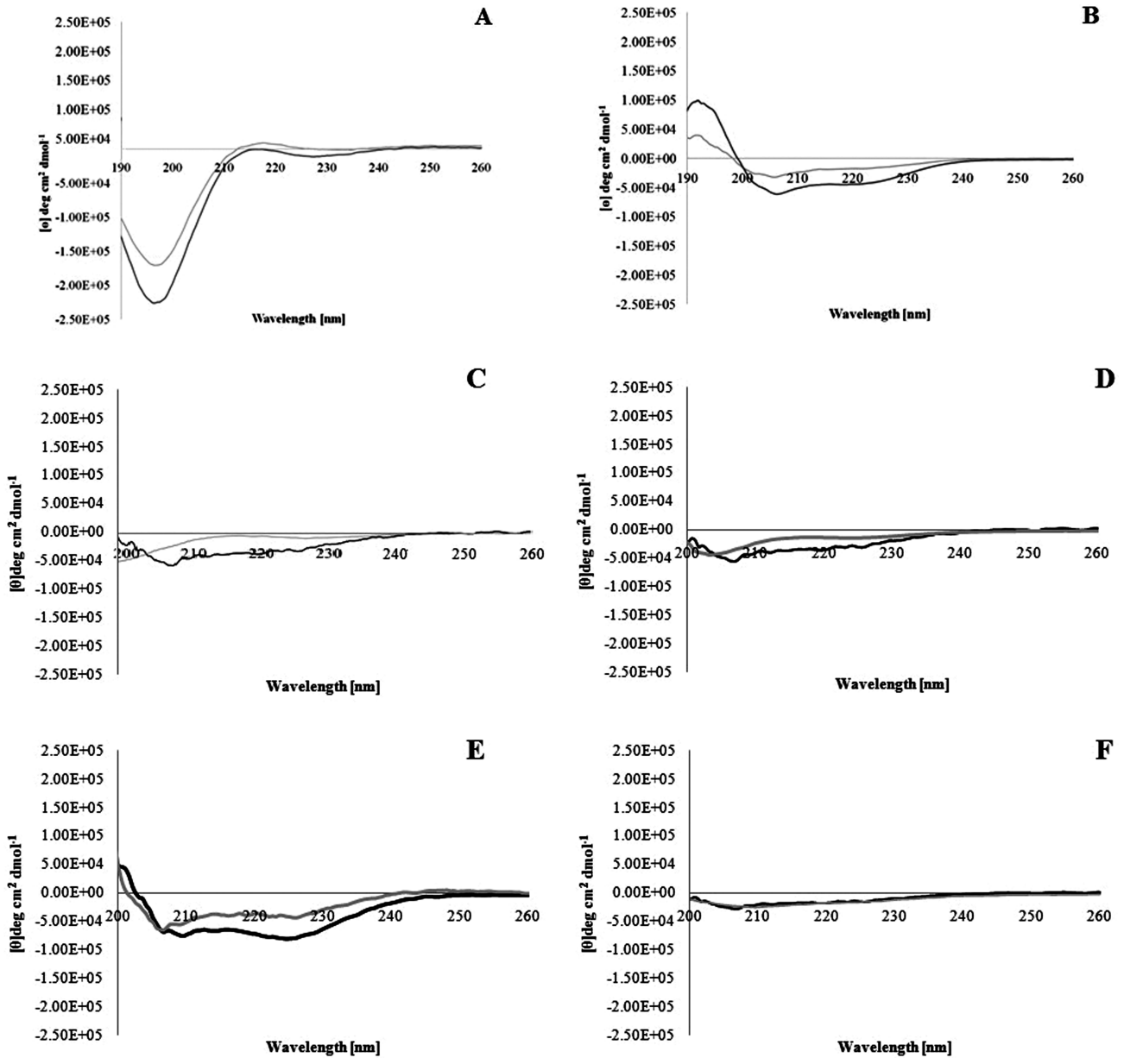

FIGURE 2: Secondary structure of modelin-5 isoforms. Circular dichroism spectra of modelin-5-COOH (gray) and modelin-5-$CONH_2$ (black) were recorded four times in water (A), a 50% TFE/water mixture (B), *E. coli* (C), DOPG (D), CL (E), and DOPE (F). Modelin-5-COOH and modelin-5-$CONH_2$ were mixed with lipid vesicles to give a peptide:lipid molar ratio of 1:100.

Table 1: Percentages of Helicity (including the standard deviations) of Modelin-5 at Peptide:Lipid Ratios of 1:100 and 1:10

			E. coli		DOPG		CL		DOPE	
peptide	H_2O	50% TFE	1:100	1:10	1:100	1:10	1:100	1:10	1:100	1:10
modelin-5-COOH	13.10 ± 0.13	52.0 ± 0.81	31.95 ± 0.41	46.89 ± 1.85	61.90 ± 0.10	76.44 ± 3.59	70.80 ± 0.57	71.22 ± 2.32	31.09 ± 0.09	45.26 ± 2.40
modelin-5-$CONH_2$	18.11 ± 0.10	100 ± 0.52	68.85 ± 0.51	90.10 ± 2.32	86.10 ± 0.09	87.35 ± 3.02	96.43 ± 0.04	98.34 ± 1.79	31.30 ± 0.67	45.36 ± 3.36

modelin-5-$CONH_2$ to FPE-labeled vesicles. At $> 50\ \mu$M, there is an increase in fluorescence in the presence of both isoforms, although maximal fluorescence induced by modelin-5-COOH remains ~30% below that of the amidated version. The binding coefficient calculated from the data obtained in Figure 4B showed that in the case of modelin-5-COOH the mean K_d was $9.6 \pm 0.16\ \mu$M (Table 2). However, in the presence of modelin-5-$CONH_2$, a slight increase in the level of binding was observed with a mean K_d of $10.1 \pm 0.21\ \mu$M (Table 2). These binding coefficients are in agreement with those observed for other synthetic antimicrobial peptides (*31*). Further analysis showed that in the case of both peptides, the Hill coefficient approximates 1 (Table 2), which along with the hyperbolic curve would suggest that the interaction of the peptide with the *E. coli* membrane was monomeric. To determine whether peptides are binding to the outer leaflet or disrupting the vesicle structure, Ca^{2+} and the ionophore calcimycin were added after the addition of the peptide. Figure 4C shows that although addition of modelin-5-COOH

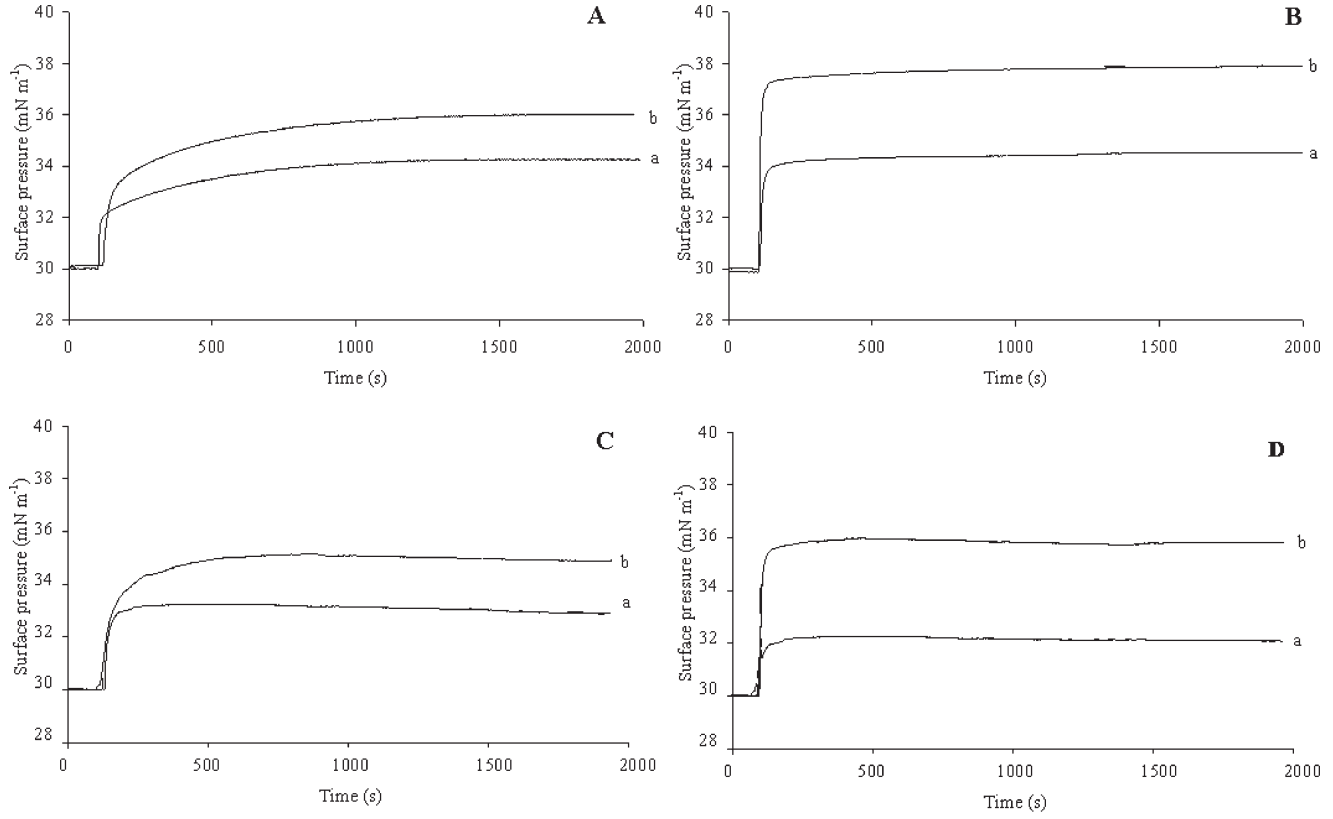

FIGURE 3: Monolayer interactions. Penetration of modelin-5-COOH (a) and modelin-5-$CONH_2$ (b) into DOPG (A), CL (B), DOPE (C), and *E. coli* lipid extract (D) monolayers. Experiments were repeated five times.

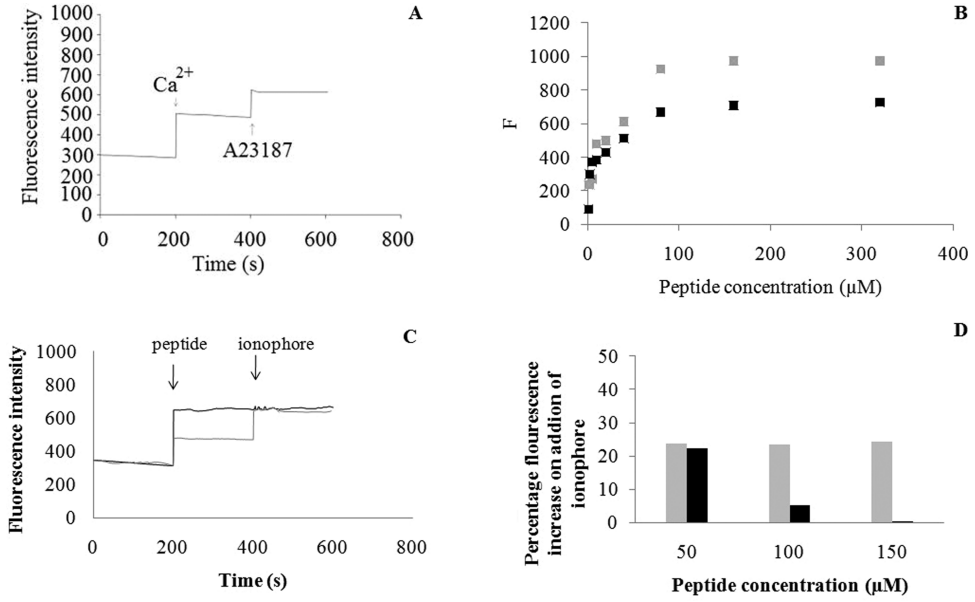

FIGURE 4: Determination of the incorporation of FPE into *E. coli* vesicles. (A) Fluorescence intensity recorded at 490 nm. At 200 s, 10 mM $CaCl_2$ was added to the system. After a further 200 s, 3.0 μM A231587 ionophore was added. (B) Binding of modelin-5-COOH (black) and modelin-5-$CONH_2$ (gray) to FPE-labeled *E. coli* vesicles. *F* is the fluorescence change in arbitrary units. (C) Determination of the incorporation of FPE into *E. coli* vesicles. The fluorescence intensity was recorded at 490 nm. At 200 s, 150 μM modelin-5-COOH (gray) and modelin-5-$CONH_2$ (black) were added to the system. After a further 200 s, 3.0 μM A231587 ionophore containing 10 mM $CaCl_2$ was added. Each experiment was repeated four times. (D) Percent fluorescence increase at peptide concentrations of 50, 100, and 150 μM after the addition of the ionophore.

at peptide concentrations of 50−150 μM induced an increase in fluorescence, the addition of the ionophore and Ca^{2+} resulted in a further increase in fluorescence, suggesting that binding had occurred on the external leaflet with Ca^{2+} gaining access to the interior only upon addition of the ionophore. While at 50 μM the addition of modelin-5-$CONH_2$ had an effect similar to that at a peptide concentration of 150 μM (Figure 4C), the addition of Ca^{2+} and the ionophore calcimycin (A23187)

Table 2: Binding Coefficients (K_d) and Hill Coefficients for Modelin-5 Isoforms in the Presence of *E. coli* Membranes

peptide	K_d (μM)	Hill coefficient
modelin-5-COOH	9.6 ± 0.16	0.9
modelin-5-$CONH_2$	10.1 ± 0.21	1.0

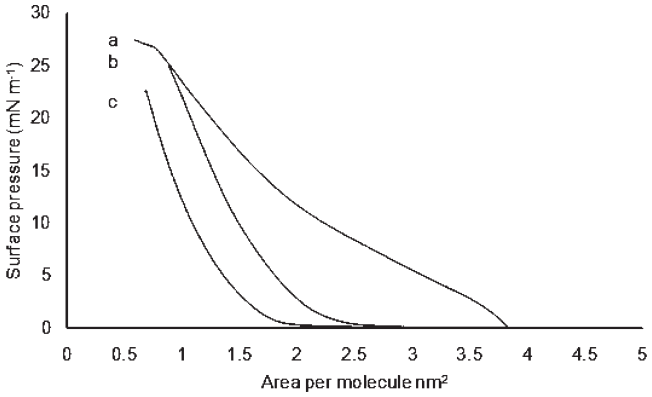

FIGURE 5: Compression isotherms derived from lipid mixtures that corresponded to membranes of *E. coli* (a) in the absence and presence of modelin-5-COOH (b) and modelin-5-$CONH_2$ (c). Experiments were repeated five times.

generated no further change in fluorescence (Figure 4D). This may well indicate that at high concentrations the amidated peptide provided access to the probe in both the internal and external leaflet.

The packing characteristics of component lipids are an important factor in determining the stability of a membrane. The packing characteristics of *E. coli* membrane mimics were investigated using thermodynamic analysis. Compression isotherms were obtained from monolayers formed from synthetic lipid mimics of *E. coli* in the presence and absence of each peptide (Figure 5). For *E. coli* model membranes, the calculated C_s^{-1} values for the isotherms indicated that all monolayers were indicative of a typical expanded lipid monolayer (*37*), with limiting areas estimated using the extrapolated area of 1.5 nm^2 in the absence of peptide, 2.1 nm^2 in the presence of modelin-5-COOH, and 3.1 nm^2 in the presence of modelin-5-$CONH_2$. The stability and binding interactions can be further investigated using the mixing enthalpy (ΔH) (Figure 6). Negative values of ΔH were observed for *E. coli* in the absence of either peptide, indicating that the monolayers were thermodynamically stable. However, in the presence of modelin-5-COOH, even though the ΔH was negative, the monolayer was not as thermodynamically stable as the control. Positive values of ΔH are observed for bacterial membrane mimics in the presence of modelin-5-$CONH_2$, indicating that there are weak interactions between the pure components and that modelin-5-$CONH_2$ has a destabilizing effect on the membrane.

DISCUSSION

Post-translational modifications such as C-terminal amidation have been thought to give enhanced biological activity to many AMPs (*23*, *38*), and our data confirm that amidating the C-terminus of modelin-5 enhances its bactericidal activity against *E. coli* approximately 10-fold. An important characteristic of AMPs is their ability to form amphiphilic structure on interaction with the membrane of pathogenic bacteria. Modelin-5 is an

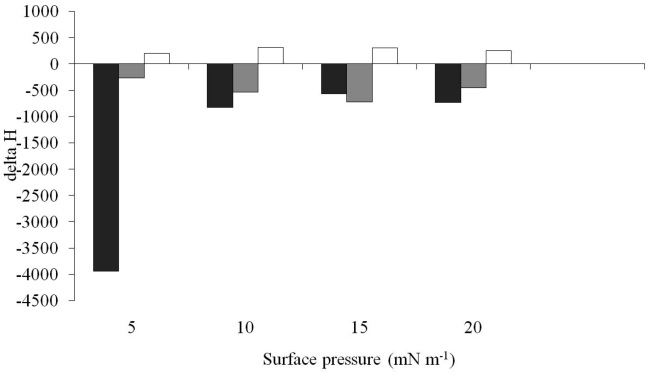

FIGURE 6: Mixing enthalpies (ΔH) of lipid monolayers at varying surface pressures. Values of ΔH were determined for monolayers formed from lipid mixtures that corresponded to membranes of *E. coli*. This parameter varied with surface pressure in the absence of peptide (black) or in the presence of modelin-5-COOH (gray) or modelin-5-$CONH_2$ (white).

amphiphilic peptide (Figure 7), and it can be seen to possess a hydrophobic arc rich in lysine residues, which may assist in the orientation of the α-helix at the membrane interface (*39*). Because modelin-5 is amphiphilic, it has therefore pronounced surface activity, inducing surface pressure increases of 23.2 and 27.1 mN/m for modelin-5-COOH and modelin-5-$CONH_2$, respectively, which is similar to the behavior observed for other amphiphilic AMPs (*34*). This amphiphilic characteristic allows them to interact with the polar−nonpolar interfacial region of cell membranes, with the hydrophobic residues perturbing the membrane interior. The similarities in surface activities (Figure 1) would imply that amidation had little effect on overall surface activity, and the data would indicate that both peptides have the potential to engage with the target membrane. Several studies have shown that for most linear AMPs the first step in their mechanism of action involves association of the membrane with the peptide located at the surface and oriented horizontal to the plane of the membrane (*1*). The surface properties of modelin-5-COOH and modelin-5-$CONH_2$ monolayers (Figure 1B) are consistent with an α-helix oriented horizontal to the air−buffer interface (*40*), which would drive the initial stages of membrane perturbation.

AMPs have been shown to display a wide range of conformations from ordered or partial α-helices and β-sheet to random coil or a mixture of these conformations (*36*). CD structural studies indicated that both peptides were unstructured in solution (Table 1) and then fold in the presence of a lipid interface. This transition can be important in generating the functional amphiphilic structure only at an asymmetric interface, with the unstructured form allowing peptides to remain in solution. This is consistent with other surface active AMPs (*36*) in which an asymmetric interface has been shown to be a requirement for amphiphilic helix formation and peptide function. To obtain further mechanistic information about the mode of action of modelin-5 analogues, CD experiments were performed in the presence of TFE, anionic lipid, zwitterionic lipid, and cell membrane lipid extract. Modelin-5-COOH was seen to adopt an α-helical structure in the presence of TFE and phospholipid membranes [52% α-helix (Table 1)], but its ability to do so was significantly weakened compared to that of the amidated form. While amidation has not enhanced the level of helix formed in solution, it has, therefore, enhanced the levels seen at a lipid interface. Coupled with the TFE data, this would imply amidation has a

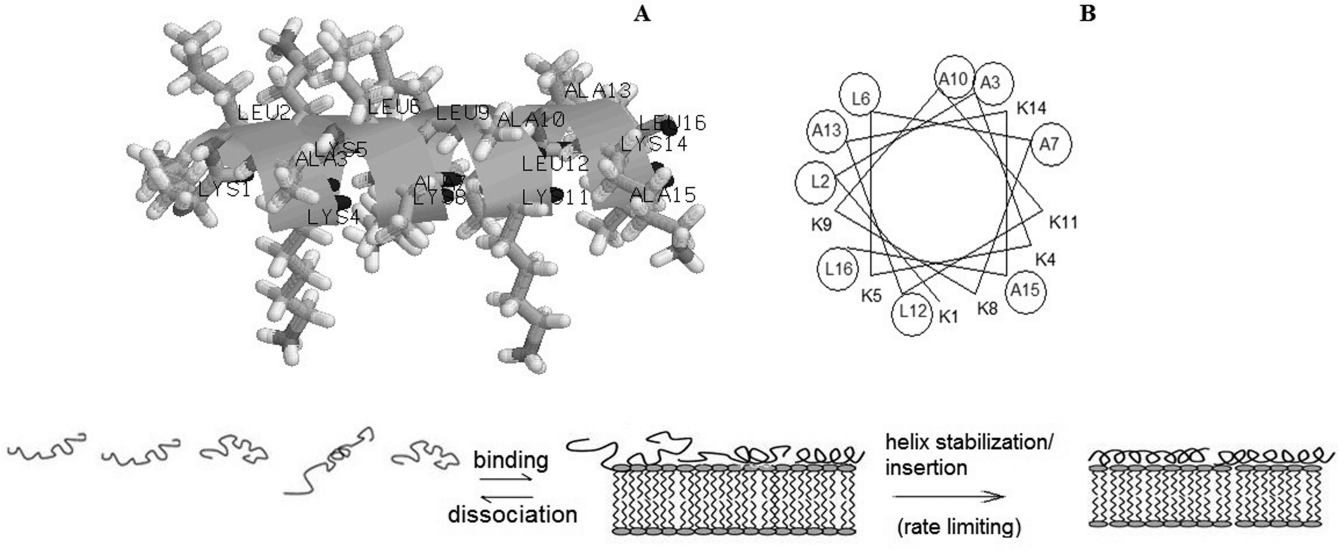

FIGURE 7: Secondary amphiphilicity of modelin-5. (A) Three-dimensional α-helical segregation of modelin-5 showing the side chains of lysine residues in the polar face. (B) Primary structure of modelin-5 represented as two-dimensional axial projections according to Schiffer (*49*) with hydrophobic residues encircled. (C) Schematic illustration of an amidated peptide interacting with the membrane. Amidation stabilizes the helix at the interface, therefore overcoming the rate-limiting step and promoting insertion into the membrane.

stabilizing effect once helix formation has occurred. The enhanced α-helical structure in the amidated form may be due to the extra hydrogen bond stabilizing the helical structure (*17*). Researchers have found similar increases in helical stability in cases where hydrogen bonding has been facilitated by helix capping motifs (*41*) or via utilization of histidine (*42*) and proline (*43*) residues. Im and Brooks (*44*) showed that for complete insertion of a 16-amino acid peptide into a membrane the structure should be more than 80% helical. Helix formation is therefore a rate-limiting step (*44*) in membrane perturbation, and this stabilization of the amidated peptide at the interface could be key to the increased activity induced by amidation of modelin-5.

It is well-established that antimicrobial peptides can differ in their selectivity for different bacteria because of the lipid composition and lipid ordering within the membrane. In this study, the effect of amidation on insertion of modelin-5 into different lipid model systems was investigated. Monolayer experiments revealed modelin-5-COOH and modelin-5-$CONH_2$ to be highly membrane active as predicted by their surface activity. To examine the charged residue distribution of modelin-5, we modeled the three-dimensional structure of the peptide using PyMOL version 0.98 (Figure 7A) and represented the peptide as a two-dimensional helical wheel (Figure 7B). It can be seen from Figure 7A that the positively charged lysine residues lie down one side of the helix, and the lysine residues define the boundary between the narrow polar and wide apolar faces of the α-helix (Figure 7B). This residue arrangement is associated with the activity of other amphiphilic antimicrobial peptides, such as aurein 1.2, which are known to exhibit high levels of monolayer penetration in the presence of an anionic lipid (*34*). In the case of modelin-5 isoforms, high levels of monolayer penetration were observed in the presence of the anionic lipids CL and PG, although lower levels of insertion were seen in the presence of zwitterionic PE, which would indicate that both peptides had a clear preference for anionic lipid. The presence of a charged lipid headgroup is known to help drive helix formation, and CD confirmed that the presence of CL induced high levels of α-helicity in modelin-5-$CONH_2$ and modelin-5-COOH (96 and 70%, respectively). It is worth noting that the modelin-5-$CONH_2$ peptide is seen to exhibit greater levels of α-helix than modelin-5-COOH (Table 1), and this enhanced propensity for helix formation is accompanied by an enhanced pressure change (Figure 3) in the presence of lipid monolayers. This becomes more apparent when considering the interaction of the peptide with *E. coli* lipid extract, which shows strong interactions with the amidated version indicative of penetration of the acyl chain region but weaker insertion of modelin-5-COOH that would be more indicative of surface binding. AMP activity is proposed to follow a two-step mechanism in which the first step involves membrane association, and given the fact that both peptides have a preference for anionic lipid and high surface activity, it would be expected that both are able to associate with the *E. coli* extract (Figure 7). The second step is thought to involve helix formation followed by membrane penetration. The lower levels of CL and PG in the *E. coli* extract appear to be sufficient to support helix formation in the case of the amidated version but less so for the nonamidated form (Table 1).

The K_d values for modelin-5 isoforms were also comparable to those of other lytic peptides such as melittin (*45*). The binding coefficient for the amidated isoform (K_d = 10.1) was slightly higher than that of the nonamidated form (K_d = 9.6), although statistical analysis of the mean K_d showed there was no significant difference between the two peptide isoforms ($T = -2.091$; $p = 0.081$). In the case of modelin-5 peptide isoforms, the Hill coefficient approximates 1, implying that these peptide membrane interactions are driven by monomeric binding events. Although the peptides had similar binding coefficients, higher helical content was observed for modelin-5-$CONH_2$ in the presence of *E. coli* membranes, which in conjunction with the monolayer data would imply more peptide was bound. Given the comparability of the binding coefficient, it may well be that once bound the impact of amidation on helix stabilization means the peptide is therefore less likely to dissociate. Baleid et al. (*46*) showed that stabilizing the helix could lead to enhanced levels of peptide at the membrane interface, which is in line with our prediction that amidation stabilizes the helix at the membrane interface, thereby allowing greater local concentrations to build up. Therefore, the data would suggest that the key differentiator

is not binding, and hence, increased efficacy caused by amidation is not likely to be driven by an increased level of targeting because of the additional charge. To investigate the mechanism of interaction of modelin isoforms, CD experiments were undertaken at varying peptide:lipid ratios. Previous studies have shown that when minimal lipid is present at a peptide:lipid ratio of 1:10 the peptide is in excess, so the peptide on the surface of the liposome is saturated and can, under these conditions, induce the formation of bicelles or micelles (*1*). A comparison of the spectra at varying peptide:lipid ratios showed that at a ratio of 1:100, in the presence of *E. coli* membranes there was a significant decrease in helicity compared to that at 1:10, for modelin-5-COOH ($T = 16.08$; $p = 0.00$) and modelin-5-$CONH_2$ ($T = 10.77$; $p = 0.00$), indicating a concentration effect. Similar effects were also seen in other cases where helicity was low, although, in contrast, Table 1 shows that where helicity is >70% an increasing peptide concentration has a limited impact on helicity, and it is likely that in those cases the membrane is already saturated.

Because both peptides lack tryptophan residues, FPE, a fluorescent probe that has been extensively studied to model peptide membrane binding (*30*, *47*, *48*), was used to monitor their ability to bind to model membranes that were mimetic with respect to *E. coli* lipid composition (Figure 4B). Modelin-5-COOH bound to the external leaflet of the membrane (Figure 4C) but appeared to be unable to provide access to the vesicle interior. Further analysis with respect to the binding of these peptides showed that at higher concentrations, in contrast to modelin-5-COOH, the amidated form is also able to provide access to the inner leaflet, which implies a greater level of membrane disruption. This is in line with previous studies, which have indicated that melittin is oriented parallel to the membrane for initial binding and at higher local concentrations is perpendicular to the membrane to allow pore formation (*45*). These results would imply that while binding occurs over a range of peptide concentrations, higher levels of peptide are required for function. Given initial binding is expected to be reversible, it may be postulated that by stabilizing the helix at the membrane interface amidation effectively increases the concentration of membrane-bound peptide enhancing the ability of the amidated form to generate pores and hence membrane damage.

Detailed analysis of the thermodynamics of the membrane allows the relationship between the peptide and packing characteristics of the membrane to be understood in more detail. The packing characteristics of *E. coli* membrane mimics were investigated using thermodynamic analysis. Figure 6 shows that ΔH was negative in the absence of peptide, which indicates that these membranes were thermodynamically stable. However, unlike in the presence of modelin-5-COOH, the amidated peptide had a destabilizing effect on the bacterial lipid monolayers [$\Delta H > 0$ (Figure 6)]. The monolayer data in Figure 3 showed deep penetration by modelin-5-$CONH_2$, supporting the suggestion that this peptide promotes toxicity in bacterial membranes using a membrane disruptive mechanism similar to the mechanisms proposed for melittin (*45*). Such penetration would be supported by the snorkeling of lysine residues on the polar face (Figure 7) to allow further penetration of the hydrophilic face.

CONCLUSIONS

In summary, it would appear from TFE data that amidation stabilizes helix formation, and this leads to enhanced levels of amphiphilic helix at a lipid interface. It is therefore proposed that there is an initial binding phase that is comparable for the amidated and nonamidated forms, with both showing a preference for anionic lipid. Once bound, the peptide could dissociate or form helical structure (Figure 7C). The stabilization of the amphiphilic helix by amidation decreases the likelihood of dissociation and supports hydrophobic partitioning at the membrane interface as seen for other AMPs such as melittin. This in turn would be predicted to provide a greater concentration of peptide at the membrane interface. This increase in the concentration of bound peptide would support pore formation or carpeting of the outer leaflet, thereby causing bilayer disruption and enhancing the efficacy of the amidated form as seen from the thermodynamic analysis. The key driver for efficacy increased by amidation would therefore appear to be the enhanced stability of the helix at an asymmetric interface and the fact amidation can therefore help overcome a rate-limiting step in lysis.

ACKNOWLEDGMENT

We thank Prof. L. H. G. Morton for support with the antimicrobial assay.

REFERENCES

1. Bechinger, B., and Lohner, K. (2006) Detergent-like actions of linear amphipathic cationic antimicrobial peptides. *Biochim. Biophys. Acta 1758*, 1529–1539.
2. Marshall, S. H., and Arenas, G. (2003) Antimicrobial peptides: A natural alternative to chemical antibiotics and a potential for applied biotechnology. *Electron. J. Biotechnol. 6*, 271–284.
3. Park, Y., and Hahm, K. S. (2005) Antimicrobial peptides (AMPs): Peptide structure and mode of action. *J. Biochem. Mol. Biol. 38*, 507–516.
4. Matsuzaki, K., Sugishita, K., Harada, M., Fujii, N., and Miyajima, K. (1997) Interactions of an antimicrobial peptide, magainin 2, with outer and inner membranes of Gram-negative bacteria. *Biochim. Biophys. Acta 1327*, 119–130.
5. Shai, Y., and Oren, Z. (2001) From "carpet" mechanism to de-novo designed diastereomeric cell-selective antimicrobial peptides. *Peptides 22*, 1629–1641.
6. Epand, R. F., Savage, P. B., and Epand, R. M. (2007) Bacterial lipid composition and the antimicrobial efficacy of cationic steroid compounds (Ceragenins). *Biochim. Biophys. Acta 1768*, 2500–2509.
7. Lohner, K., and Prenner, E. J. (1999) Differential scanning calorimetry and X-ray diffraction studies of the specificity of the interaction of antimicrobial peptides with membrane-mimetic systems. *Biochim. Biophys. Acta 1462*, 141–156.
8. Andreu, D., and Rivas, L. (1998) Animal antimicrobial peptides: an overview. *Biopolymers 47*, 415–433.
9. Boland, M. P., and Separovic, F. (2006) Membrane interactions of antimicrobial peptides from Australian tree frogs. *Biochim. Biophys. Acta 1758*, 1178–1183.
10. Gehman, J. D., Luc, F., Hall, K., Lee, T. H., Boland, M. P., Pukala, T. L., Bowie, J. H., Aguilar, M. I., and Separovic, F. (2008) Effect of antimicrobial peptides from Australian tree frogs on anionic phospholipid membranes. *Biochemistry 47*, 8557–8565.
11. Mor, A., and Nicolas, P. (1994) The NH2-terminal α-helical domain 1−18 of dermaseptin is responsible for antimicrobial activity. *J. Biol. Chem. 269*, 1934–1939.
12. Kreil, G. (1973) Biosynthesis of melittin, a toxic peptide from bee venom. Amino-acid sequence of the precursor. *Eur. J. Biochem. 33*, 558–566.
13. Callaway, J. E., Lai, J., Haselbeck, B., Baltaian, M., Bonnesen, S. P., Weickmann, J., Wilcox, G., and Lei, S. P. (1993) Modification of the C terminus of cecropin is essential for broad-spectrum antimicrobial activity. *Antimicrob. Agents Chemother. 37*, 1614–1619.
14. Bulet, P., Stocklin, R., and Menin, L. (2004) Anti-microbial peptides: From invertebrates to vertebrates. *Immunol. Rev. 198*, 169–184.
15. Moore, A. J., Devine, D. A., and Bibby, M. C. (1994) Preliminary experimental anticancer activity of cecropins. *Pept. Res. 7*, 265–269.
16. White, S. H., and Wimley, W. C. (1998) Hydrophobic interactions of peptides with membrane interfaces. *Biochim. Biophys. Acta 1376*, 339–352.

17. Shalev, D. E., Mor, A., and Kustanovich, I. (2002) Structural consequences of carboxyamidation of dermaseptin S3. *Biochemistry 41*, 7312–7317.
18. Lee, K. H., Hong, S. Y., Oh, J. E., Kwon, M., Yoon, J. H., Lee, J., Lee, B. L., and Moon, H. M. (1998) Identification and characterization of the antimicrobial peptide corresponding to C-terminal β-sheet domain of tenecin 1, an antibacterial protein of larvae of *Tenebrio molitor*. *Biochem. J. 334* (Part 1), 99–105.
19. Mor, A., Hani, K., and Nicolas, P. (1994) The vertebrate peptide antibiotics dermaseptins have overlapping structural features but target specific microorganisms. *J. Biol. Chem. 269*, 31635–31641.
20. Falla, T. J., and Hancock, R. E. (1997) Improved activity of a synthetic indolicidin analog. *Antimicrob. Agents Chemother. 41*, 771–775.
21. Giangaspero, A., Sandri, L., and Tossi, A. (2001) Amphipathic α helical antimicrobial peptides. *Eur. J. Biochem. 268*, 5589–5600.
22. Bessalle, R., Gorea, A., Shalit, I., Metzger, J. W., Dass, C., Desiderio, D. M., and Fridkin, M. (1993) Structure-function studies of amphiphilic antibacterial peptides. *J. Med. Chem. 36*, 1203–1209.
23. Owen, D. R. (2005) Short bioactive peptides. U.S. Patent 6875744, Helix BioMedix, Inc.
24. Bligh, E. G., and Dyer, W. J. (1959) A rapid method of total lipid extraction and purification. *Can. J. Med. Sci. 37*, 911–917.
25. Seeling, A. (1987) Local anesthetics and pressure: A comparison of dibucaine binding to lipid monolayers and bilayers. *Biochim. Biophys. Acta 899*, 196–204.
26. Alminana, N., Alsina, M. A., Ortiz, A., and Reig, F. (2004) Comparative physicochemical study of SIKVAV peptide and its retro and retro-enantio analogues. *Colloids Surf., A 249*, 19–24.
27. Todd, J. (1963) Introduction to the Constructive Theory of Functions, Academic Press, New York.
28. Quickenden, T. I., and Tan, G. K. (1974) Random packing in two dimensions and the structure of monolayers. *J. Colloid Interface Sci. 48*, 382–393.
29. Forood, B., Feliciano, E. J., and Nambiar, K. P. (1993) Stabilization of α-helical structures in short peptides via end capping. *Proc. Natl. Acad. Sci. U.S.A. 90*, 838–842.
30. Wall, J., Golding, C. A., Van Veen, M., and O'Shea, P. (1995) The use of fluoresceinphosphatidylethanolamine (FPE) as a real-time probe for peptide-membrane interactions. *Mol. Membr. Biol. 12*, 183–192.
31. Moreno, M. R., Guillen, J., Perez-Berna, A. J., Amoros, D., Gomez, A. I., Bernabeu, A., and Villalain, J. (2007) Characterization of the interaction of two peptides from the N terminus of the NHR domain of HIV-1 gp41 with phospholipid membranes. *Biochemistry 46*, 10572–10584.
32. Dennison, S. R., Morton, L. H., Shorrocks, A. J., Harris, F., and Phoenix, D. A. (2009) A study on the interactions of Aurein 2.5 with bacterial membranes. *Colloids Surf., B 68*, 225–230.
33. Hancock, R. E., and Diamond, G. (2000) The role of cationic antimicrobial peptides in innate host defences. *Trends Microbiol. 8*, 402–410.
34. Dennison, S. R., Harris, F., and Phoenix, D. A. (2007) The interactions of aurein 1.2 with cancer cell membranes. *Biophys. Chem. 127*, 78–83.
35. Sospedra, P., Haro, I., Alsina, M. A., Reig, F., and Mestres, C. (1999) Physicochemical interaction of a lipophilic derivative of HAV antigen VP3(110−121) with lipid monolayers. *Mater. Sci. Eng., C 8−9*, 543–549.
36. Maget-Dana, R. (1999) The monolayer technique: A potent tool for studying the interfacial properties of antimicrobial and membranelytic peptides and their interactions with lipid membranes. *Biochim. Biophys. Acta 1462*, 109–140.
37. Davies, J. T., and Rideal, E. K. (1963) Interfacial Phenomena, 2nd ed., Academic Press, New York.
38. Cerovsky, V., Slaninova, J., Fucik, V., Hulacova, H., Borovickova, L., Jezek, R., and Bednarova, L. (2008) New potent antimicrobial peptides from the venom of Polistinae wasps and their analogs. *Peptides 29*, 992–1003.
39. Marcotte, I., Wegener, K. L., Lam, Y. H., Chia, B. C., de Planque, M. R., Bowie, J. H., Auger, M., and Separovic, F. (2003) Interaction of antimicrobial peptides from Australian amphibians with lipid membranes. *Chem. Phys. Lipids 122*, 107–120.
40. Ambroggio, E. E., Separovic, F., Bowie, J., and Fidelio, G. D. (2004) Surface behaviour and peptide-lipid interactions of the antibiotic peptides, Maculatin and Citropin. *Biochim. Biophys. Acta 1664*, 31–37.
41. Parker, M. H., and Hefford, M. A. (1998) Introduction of potential helix-capping residues into an engineered helical protein. *Biotechnol. Appl. Biochem. 28* (Part 1), 69–76.
42. Armstrong, K. M., and Baldwin, R. L. (1993) Charged histidine affects α-helix stability at all positions in the helix by interacting with the backbone charges. *Proc. Natl. Acad. Sci. U.S.A. 90*, 11337–11340.
43. Mason, A. J., Martinez, A., Glaubitz, C., Danos, O., Kichler, A., and Bechinger, B. (2006) The antibiotic and DNA-transfecting peptide LAH4 selectively associates with, and disorders, anionic lipids in mixed membranes. *FASEB J. 20*, 320–322.
44. Im, W., and Brooks, C. L., III (2005) Interfacial folding and membrane insertion of designed peptides studied by molecular dynamics simulations. *Proc. Natl. Acad. Sci. U.S.A. 102*, 6771–6776.
45. van den Bogaart, G., Guzman, J. V., Mika, J. T., and Poolman, B. (2008) On the mechanism of pore formation by melittin. *J. Biol. Chem. 283*, 33854–33857.
46. Beleid, R., Douglas, D., Kneteman, N., and Kaur, K. (2008) Helical peptides derived from lactoferrin bind hepatitis C virus envelope protein E2. *Chem. Biol. Drug Des. 72*, 436–443.
47. Hawrani, A., Howe, R. A., Walsh, T. R., and Dempsey, C. E. (2010) Thermodynamics of RTA3 peptide binding to membranes and consequences for antimicrobial activity. *Biochim. Biophys. Acta 1798*, 1254–1262.
48. O'Toole, P. J., Morrison, I. E., and Cherry, R. J. (2000) Investigations of spectrin-lipid interactions using fluoresceinphosphatidylethanolamine as a membrane probe. *Biochim. Biophys. Acta 1466*, 39–46.
49. Schiffer, M., and Edmundson, A. B. (1967) Use of helical wheels to represent the structures of proteins and to identify segments with helical potential. *Biophys. J. 7*, 121–135.